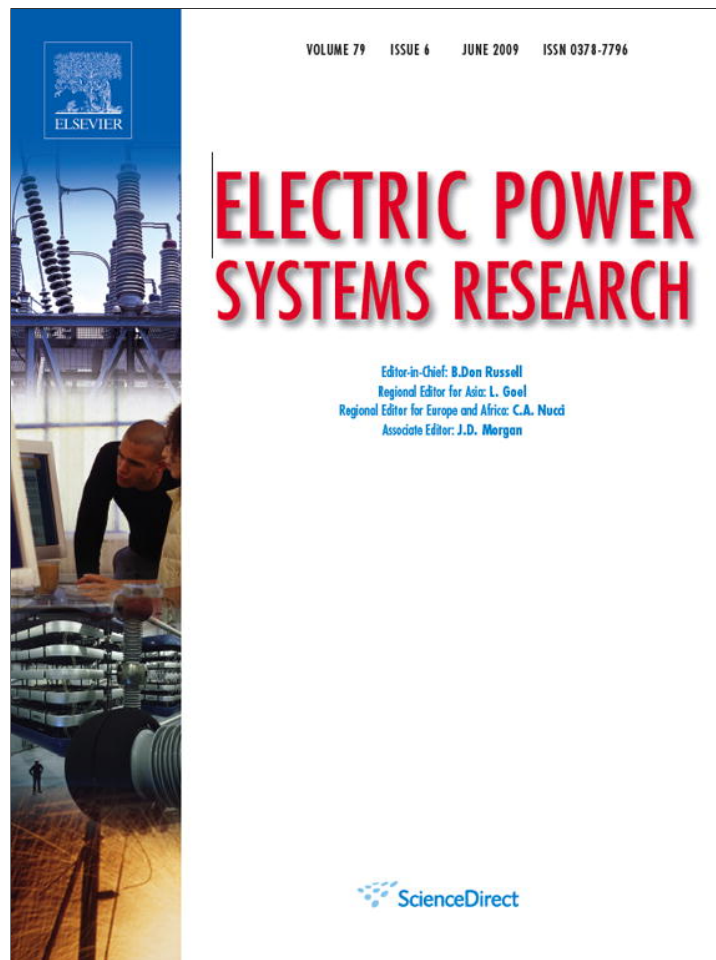


Provided for non-commercial research and education use.
Not for reproduction, distribution or commercial use.



This article appeared in a journal published by Elsevier. The attached copy is furnished to the author for internal non-commercial research and education use, including for instruction at the authors institution and sharing with colleagues.

Other uses, including reproduction and distribution, or selling or licensing copies, or posting to personal, institutional or third party websites are prohibited.

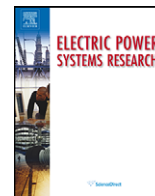
In most cases authors are permitted to post their version of the article (e.g. in Word or Tex form) to their personal website or institutional repository. Authors requiring further information regarding Elsevier's archiving and manuscript policies are encouraged to visit:

<http://www.elsevier.com/copyright>



Contents lists available at ScienceDirect

Electric Power Systems Research

journal homepage: www.elsevier.com/locate/epsr

Demand and generation cost uncertainty modelling in power system optimization studies

Bruno André Gomes, João Tomé Saraiva*

INESC Porto and Departamento de Engenharia Electrotécnica e Computadores, Faculdade de Engenharia da Universidade do Porto, FEUP, Campus da FEUP Rua Roberto Frias 378, 4200 465 Porto, Portugal

ARTICLE INFO

Article history:

Received 19 March 2008

Received in revised form 10 July 2008

Accepted 19 December 2008

Available online 30 January 2009

Keywords:

Uncertainties

Generation cost uncertainties

Demand uncertainties

Fuzzy models

Multiparametric linear programming

ABSTRACT

This paper describes the formulations and the solution algorithms developed to include uncertainties in the generation cost function and in the demand on DC OPF studies. The uncertainties are modelled by trapezoidal fuzzy numbers and the solution algorithms are based on multiparametric linear programming techniques. These models are a development of an initial formulation detailed in several publications co-authored by the second author of this paper. Now, we developed a more complete model and a more accurate solution algorithm in the sense that it is now possible to capture the widest possible range of values of the output variables reflecting both demand and generation cost uncertainties. On the other hand, when modelling simultaneously demand and generation cost uncertainties, we are representing in a more realistic way the volatility that is currently inherent to power systems. Finally, the paper includes a case study to illustrate the application of these models based on the IEEE 24 bus test system.

© 2008 Elsevier B.V. All rights reserved.

1. Introduction

The treatment of uncertainties has been a concern among the power systems community for a long time. This fact is clear with the development of several models integrating uncertainty for instance under the form of probabilistic models. This is the case of reliability models and also regarding power-flow approaches. In recent years, power systems went through a restructuring process that determined the unbundling of the traditional vertically integrated companies in different agents and providers that can be grouped in several activities as generation, transmission, distribution and retailing as well as in several coordination activities including the market operator, the system operator and the regulatory boards. The extreme activities of this value chain, generation and retailing, are typically provided through competitive mechanisms, while wiring transmission and distribution activities are framed in terms of monopoly-regulated basis.

One of the consequences of the unbundling of power systems and the introduction of competition in some areas is related with the more volatile environment that companies and consumers are now facing. Apart from that, the cost of fuels is more volatile than in the past and it is affected by very subjective factors that can determine quick changes on the market prices. This increased volatility

affecting a number of factors contributes to reduce the available history regarding the behavior of those factors and parameters and so it is more important to formalize the knowledge provided by planners and experts using human language.

At this point, it is important to recall that within the probabilistic models framework, we admit that a phenomenon is reproducible, which means that the rules governing it remain the same along time. Given the randomness of this type of phenomenon, probabilistic models rely on the observation of a large number of events from which one can derive probabilistic distributions. In fact, in periods of large volatility affecting not only the numerical values of several parameters but also the legislation and regulations determining power system operation as well the change of paradigm affecting the whole industry, it becomes important to develop new models able to integrate a different type of uncertainty. In this sense, fuzzy models were conceived to represent the uncertainty inherent, for instance, to a large number of expressions of our language. In fact, expressions as “large”, “more or less” or “approximately” do not result from the repetitive simulation of the same phenomenon but express the past experience of the user and his subjective evaluation. The formalization of this type of knowledge and its integration in several power system models can therefore contribute to enlarge the insight of the users regarding the possible ways a power system will be operated reflecting the specified uncertainties.

During the 1990s, a number of contributions referred in Section 2 were published that aimed at including in several power system operation and planning models demand uncertainties represented by trapezoidal fuzzy numbers. In line with these concerns,

* Corresponding author. Tel.: +351 22 2094230; fax: +351 22 2094150.
E-mail addresses: bgomes@inescporto.pt (B.A. Gomes), jsaraiva@fe.up.pt (J.T. Saraiva).

we recently resumed this area of research in order to develop more complete and more accurate models. In this sense, we are now considering not only demand uncertainties but also generation cost uncertainties, both represented by trapezoidal fuzzy numbers, defined in Section 3. This means we are now able to investigate the consequences for power system operation from having simultaneously fuzzy representations of some nodal demands and some generation costs. On the other hand, the original solution algorithm developed back in the 1990s adopted a simplified approach to build the membership functions for generations, branch flows and power not supplied. As a consequence of this simplified approach, the range of possible values obtained at that time could, in some cases, not correspond to the widest possible behavior of the problem outputs. In this paper, we describe the use of linear multiparametric optimization techniques that ensure that the whole uncertainty space is covered so that we are accurately transferring data uncertainty onto the results of the optimization problems.

Following these ideas, this paper is structured as follows. After this introduction, Section 2 briefly addresses the integration of uncertainties in several power system studies, both using probabilistic and fuzzy set models. Section 3 presents the fundamental concepts of fuzzy set theory useful to fully understand the remaining sections. Section 4 details the original fuzzy DC optimal power flow problem as well as the new formulations we have developed. Section 5 describes the developed solution algorithms and Section 6 presents results obtained with a case study based on the IEEE 24 bus test system. Finally, Section 7 draws the most relevant conclusions.

2. Dealing with uncertainty in power-flow and optimal power-flow studies

Probabilistic models were the traditional approach to incorporate uncertainties in several power system studies. The treatment of uncertainties and their integration namely in power-flow studies started back in the 1970s with the publication of the models described in references [1–5]. These papers describe the main concepts related with this problem as well as the initially developed algorithms using convolution techniques, the DC model and different linearized versions of the AC power-flow problem. In general, these approaches aimed at translating to the results of traditional power flows the uncertainties specified in data under the form of probabilistic distributions. Due to the linearizations adopted in several of these models, it was soon realized that the results were affected by errors that would eventually be larger in the tails of the output distributions. Concerned with this problem, reference [6] describes the use of the Monte Carlo simulation technique to evaluate the accuracy of the results and references [7,8] propose the use of several linearization points to build partial probability distributions that, at the end, would be aggregated to provide the final outputs. This approach was conceived as a way to reduce the errors in the tails of the output distributions.

These models constitute the basic approaches developed to incorporate probabilistic data in power-flow problems. In this sense, in subsequent years, some other contributions were published to enrich the previous models or to give them an increased realism. References [9,10] are two examples of this kind of contributions when considering network outages and operation constraints used to constrain the power-flow results. Finally, reference [11] describes a new approach to the probabilistic power-flow problem directed to the construction of the branch flow distributions in order to get useful information to be used in transmission investment planning problems.

Apart from probabilistic power-flow models, the literature also includes a few references addressing the integration of probabilistic data in optimal power flow models. In this scope, reference [12] admits that the demand has a normal distribution probability

function and describes the computation of expected values of the output variables. Reference [13] considers that the demand is represented by a vector of random correlated variables so that nodal dependencies can be modelled. This paper adopts the first-order second-moment method in order to get the statistical properties of the output variables reflecting data uncertainty. Finally, reference [14] describes the use of a cumulant-based approach to compute the output probability distributions while comparing these results with the ones obtained by Monte Carlo simulations as a way to evaluate their accuracy.

Apart from probabilistic models, the difficulty in forecasting the future behavior of several parameters and data has long been addressed using scenario analysis and sensitivity approaches. As an example, reference [15] describes an approach to investigate how the optimal operation point of a power system can be affected by changing input data. In this case, the authors consider changes in the active or reactive load at a specified bus or at the thermal limit of a branch and adopt a Lagrange-based formulation to obtain these sensitivities.

In the early 1990s, fuzzy set models started to be applied to several power systems problems, namely in operation planning models recognizing that in some cases the uncertainty we want to deal with has not a probabilistic nature or we simply do not have enough data to build reliable probabilistic distributions. In some situations, the uncertainty is inherently related with human language, since judgments using such expressions as “more or less”, “larger than”, “approximately” are not a consequence of the repetition of an experience under the same conditions but are, in fact, a result of the past experience of the planner that integrates information and produces a judgment that, in any case, reflects his subjectivity. The mathematical formalization of this knowledge became an important aspect in different scientific areas as a way to express the volatility increasingly present in our world. Regarding power-flow problems, reference [16] details the first DC and AC models admitting that at least one generation and demand are modelled by fuzzy numbers. As a result, voltages and branch flows are now represented by fuzzy numbers expressing the possible behavior of the system given the specified uncertainties.

A subsequent step was given with references [17,18] with the development of a Fuzzy DC OPF model admitting that at least a demand was represented by a fuzzy number. As a result, generations, branch flows and if necessary power not supplied (PNS) are obtained as fuzzy representations translating data uncertainty. Afterwards, this approach was integrated in a Monte Carlo simulation [19] as way to obtain estimates of the expected value of the output variables reflecting fuzzy loads and reliability equipment data modelled with the usual probability-based approaches. In this sense, the model in reference [19] has a hybrid nature when aggregating fuzzy and probabilistic models. The referred Fuzzy DC OPF model was also integrated in a methodology to identify the most adequate expansion plan so that the risk of not being able to meet the demand gets reduced while accommodating the inherent uncertainty [20]. Finally, reference [21] presents the basic concepts related with the simultaneous modelling of generation cost and demand uncertainties. These concepts, the mathematical formulations and the developed solution algorithms will now be fully detailed in this paper.

3. Fuzzy set basics

A fuzzy set \tilde{A} is defined as a set of ordered pairs (1) in which the first element, x_1 , corresponds to an element of the universe X under analysis and the second is the membership degree of that element to the fuzzy set, $\mu_{\tilde{A}}(x_1)$. In normalized fuzzy sets, the membership degree takes values in $[0.0;1.0]$ and reflects the degree of compatibility of the elements of X with the proposition defining the fuzzy

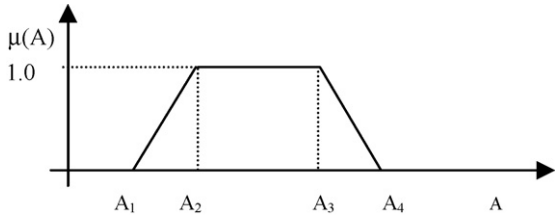


Fig. 1. Trapezoidal fuzzy number.

set. These membership degrees can be interpreted as a membership function $\mu_{\tilde{A}}(x)$ that assigns a membership degree to each element x .

$$\tilde{A} = \{(x_1; \mu_{\tilde{A}}(x_1)), x_1 \in X\} \quad (1)$$

A particular class of fuzzy sets corresponds to fuzzy numbers. A fuzzy set \tilde{A} is classified as a fuzzy number if it is a convex fuzzy set defined on the real line R such that its membership function is piecewise continuous. As an example, Fig. 1 represents the membership function of a trapezoidal fuzzy number in which the membership degree is maximum in $[A_2; A_3]$ and decreases from 1.0 to 0.0 from A_2 to A_1 and from A_3 to A_4 . Regarding this type of numbers and given the particular form of the membership function, they are uniquely defined if the values of A_1, A_2, A_3 and A_4 are known. This number is then usually written as $(A_1; A_2; A_3; A_4)$.

An α -level set or an α -cut of a fuzzy set \tilde{A} is defined in X as the hard set A_α obtained from \tilde{A} for each $\alpha \in [0.0; 1.0]$ according to (2). As a result of this definition, the 0.0-cut of the fuzzy number in Fig. 1 is the interval $[A_1; A_4]$, while the 1.0-cut is given by the interval $[A_2; A_3]$.

$$A_\alpha = \{x_1 \in X : \mu_{\tilde{A}}(x_1) \geq \alpha\} \quad (2)$$

Finally, the central value of a fuzzy number corresponds to the mean value of the 1.0-cut. Regarding the trapezoidal fuzzy number in Fig. 1, the central value of \tilde{A} , A^{ctr} , is given by (3).

$$A^{ctr} = \frac{A_2 + A_3}{2} \quad (3)$$

4. Problem formulation

4.1. Fuzzy optimal power-flow model

References [17,18] describe the original Fuzzy DC OPF model in which we admitted that uncertainties only affected the demand vector. This formulation used the DC model to represent the operation of the transmission system and the solution algorithm is presented in Fig. 2.

This algorithm starts by solving a deterministic DC OPF in which we substituted the fuzzy demands by the corresponding central values. This leads to the linear optimization problem (4)–(8).

$$\min f = \sum c_k P_{gk} + G \sum PNS_k \quad (4)$$

$$\text{s.t.} \quad \sum P_{gk} + \sum PNS_k = \sum P_k^{ctr} \quad (5)$$

$$P_{gk}^{min} \leq P_{gk} \leq P_{gk}^{max} \quad (6)$$

$$PNS_k \leq P_k^{ctr} \quad (7)$$

$$P_b^{min} \leq \sum a_{bk} (P_{gk} + PNS_k - P_k^{ctr}) \leq P_b^{max} \quad (8)$$

This problem minimizes the generation cost given that P_{gk} is the generation in bus k having cost c_k , PNS_k is the power not supplied in bus k and the coefficient G penalizes power not supplied. In this formulation, P_{gk}^{min} , P_{gk}^{max} , P_b^{min} and P_b^{max} are the minimum and maximum generation and branch limits, a_{bk} is the DC sensitivity

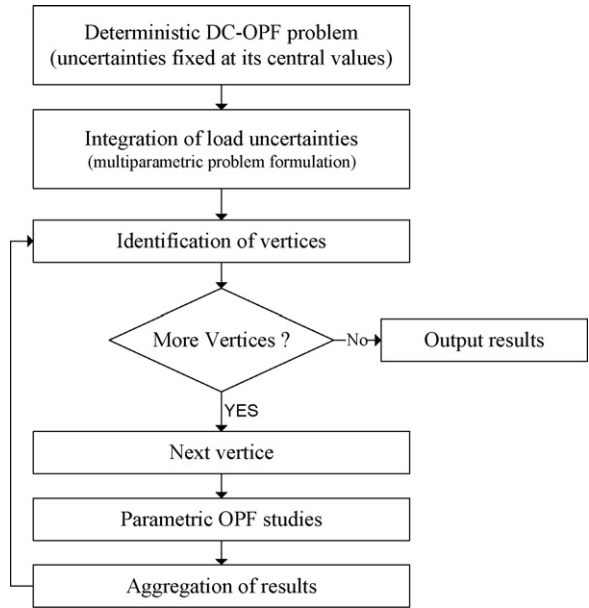


Fig. 2. Algorithm of the original fuzzy DC optimal power flow model.

coefficient of the flow in branch b regarding the injected power in bus k and P_k^{ctr} is the central value of the load in node k .

After solving this initial deterministic problem, we get an initial optimal and feasible solution. However, the demand is affected by uncertainty and so this optimal and feasible basis can be no longer feasible for several combinations of the uncertainties. In order to take this into account, we introduce parameters Δ_k related with load uncertainties in the previous problem so that we formulate the multiparametric problem given by (9)–(11). In this problem, b and b' are vectors representing the right-hand side terms of the constraints given that some of them are independent and some others depend on the parameters Δ_k used to model load uncertainties.

$$\min f = c^t X \quad (9)$$

$$\text{s.t.} \quad AX = b + b'(\Delta_k) \quad (10)$$

$$\Delta_{k1} \leq \Delta_k \leq \Delta_{k4} \quad (11)$$

The solution algorithm described in references [17,18] identifies vertices of the hypervolume defined by (11) and then solves a set of parametric linear programming problems in order to vary the load from the set of central values to the values associated with each of these vertices. While solving these parametric problems, one builds partial membership functions for the generations, branch flows and PNS. The final membership function of each of these variables is obtained applying the fuzzy union operator on those partial results.

Accordingly, this algorithm transforms the multiparametric problem (9)–(11) into a set of parametric problems and this represents a simplification that may lead to inaccuracies when obtaining the final results. This means that in several problems we could obtain membership functions that would not capture the widest possible behavior of each variable. In this paper, we deal with the multiparametric problem by itself and we enlarge the fuzzy optimal power flow problem considering not only demand uncertainties but also generation cost uncertainties.

4.2. Condensed formulations

In a condensed way, the DC OPF problem admitting that at least one load is represented by a trapezoidal fuzzy number as the one sketched in Fig. 1 can be formulated by (12) and (13). In this case, the vector of the right-hand side terms of the constraints has at least one

element represented by a trapezoidal fuzzy number representing a demand. As a result, the output variables of this problem (generations, branch flows and PNS) will also be represented by fuzzy numbers reflecting data uncertainty.

$$\min f = c^t \tilde{X} \quad (12)$$

$$\text{s.t. } A\tilde{X} \leq \tilde{b} \quad (13)$$

A second problem corresponds to the integration of generation cost uncertainties modelled by trapezoidal fuzzy numbers. This problem can be formulated by (14) and (15). In this case, the generation costs are affected by uncertainties leading to uncertainties in the output variables.

$$\min f = \tilde{c}^t \tilde{X} \quad (14)$$

$$\text{s.t. } A\tilde{X} \leq b \quad (15)$$

Finally, if we now consider both generator cost and load uncertainties modelled by trapezoidal fuzzy numbers, then we get the condensed formulations (16) and (17). In the next section, we will detail the solution algorithms that were developed to solve these three problems.

$$\min f = \tilde{c}^t \tilde{X} \quad (16)$$

$$\text{s.t. } A\tilde{X} \leq \tilde{b} \quad (17)$$

5. Solution algorithms

5.1. General aspects

The development of electricity markets and the volatility of fuel prices place a new emphasis on power system planning and operation as well as on the economic liquidity of the markets. Recognizing these concerns, the new fuzzy optimal power flow (NFOPF) approach aims at, in the first place, extending the original concept by translating to the results not only load uncertainties but also generation costs uncertainties. Secondly, since computational resources are nowadays more powerful than in past, the NFOPF also enables obtaining a more accurate solution for this type of problems, since it adopts linear multiparametric optimization techniques. The application of these techniques leads to the identification of a number of critical regions covering all the uncertainty space, meaning that we are effectively covering all the combinations of values of the parameters affected by uncertainties. This has an important consequence, given that we can now obtain more accurate membership functions in the sense they represent the widest possible behavior of each variable. The original FOPF model described in Section 4 only runs a number of linear parametric studies, eventually leading to narrower membership functions when compared with the real ones.

The algorithms used to solve these linear multiparametric problems were originally proposed by Gal [22]. Starting at the initial optimal and feasible solution of the deterministic optimization problem as stated by (4)–(8), these algorithms identify the critical regions in the uncertainty space. This means that they search all the combinations of values of the parameters affected by uncertainties for which there is an optimal and feasible basis. When running this process, we are extending the optimality and feasibility conditions ((18) and (19), respectively) so that they become function of Φ_k (parameters modelling generation cost uncertainties) or Δ_k (parameters modelling load uncertainties). Then, starting at the optimal and feasible solution of the initial deterministic DC OPF problem and considering each of these conditions, we find the set of other optimal and feasible solutions, provided they are valid in some region of the uncertainty space. These regions are called critical regions and this process is conducted by pivoting over the initial

basis as well as over all the new ones identified during the search process.

From a mathematical point of view, let B be an optimal and feasible basis, ρ the index for the corresponding set of basic variables, A the columns of the non-basic variables in the simplex tableau, C_0 the cost vector of the basic variables and C^T the cost vector of the non-basic variables. The optimality and feasibility conditions for a minimization linear problem can then be defined in terms of Φ_k and Δ_k by (18) and (19).

$$C^T(\Phi_k) - C_0^T B_\rho^{-1} A = (c + c'(\Phi_k)) - C_0^T B_\rho^{-1} A \geq 0 \quad (18)$$

$$B_\rho^{-1} b(\Delta_k) = B_\rho^{-1} (b + b'(\Delta_k)) \geq 0 \quad (19)$$

Since the dual solution does not depend on Δ_k for right-hand side parametrization, a critical region, i.e., a region in the uncertainty space where B remains optimal and feasible, can be uniquely defined by the conditions in (19). In a similar way, since the primal solution does not depend on Φ_k for cost parametrization, a critical region can be defined by the conditions given by (18). Apart from these conceptual aspects, two optimal and feasible basis, B_1 and B_2 , are considered neighbor ones if and only if one can pass from B_1 to B_2 performing one dual pivot step in case of right-hand side parametrization or one primal pivot step in case of cost vector parametrization.

As a final comment, the ultimate objective to attain when solving a multiparametric optimization problem is to find all possible optimal solutions, their corresponding optimal values and critical regions, which can be defined as a closed nonempty polyhedron, that is, a set of linear inequalities established in terms of Δ , of Φ , or in terms of both. Mathematically, this set of constraints can be expressed as the equivalent set of non-redundant constraints, which in turn can be identified through a non-redundant test for linear inequalities, like the one proposed by Gal [22].

5.2. Integration of load uncertainties

Fig. 3 presents the algorithm of the NFOPF. Similarly to the algorithm described in Section 4, in this new approach, it is also performed an initial deterministic DC OPF problem (4)–(8) to identify a feasible and optimal solution associated to the central values of the fuzzy load representations. In the second place, the parameters modelling load uncertainties are included in the original optimization problem leading to the problem (20)–(24).

$$\min f = \sum c_k P g_k + G \sum \text{PNS}_k \quad (20)$$

$$\text{s.t. } \sum P g_k + \sum \text{PNS}_k = \sum P l_k^{\text{ctr}} + \sum \Delta_k \quad (21)$$

$$P g_k^{\min} \leq P g_k \leq P g_k^{\max} \quad (22)$$

$$\text{PNS}_k \leq P l_k^{\text{ctr}} + \Delta_k \quad (23)$$

$$P b^{\min} \leq \sum a_{bk} (P g_k + \text{PNS}_k - (P l_k^{\text{ctr}} + \Delta_k)) \leq P b^{\max} \quad (24)$$

Following the algorithm in Fig. 3, we will now identify a set of non-redundant constraints defining new critical regions considering the inequalities associated with the feasibility condition (19). If there are no non-redundant constraints, the algorithm stops indicating that the current basis is feasible in the whole uncertainty space. Otherwise, it performs a dual pivoting over the initial optimal and feasible solution to identify new critical regions. This process is repeated until no non-redundant constraints exist or until all identified critical regions correspond to already known ones. When this is over, all the uncertainty space was covered and we identified all critical regions in which a base B of the problem (20)–(24) remains feasible and optimal.

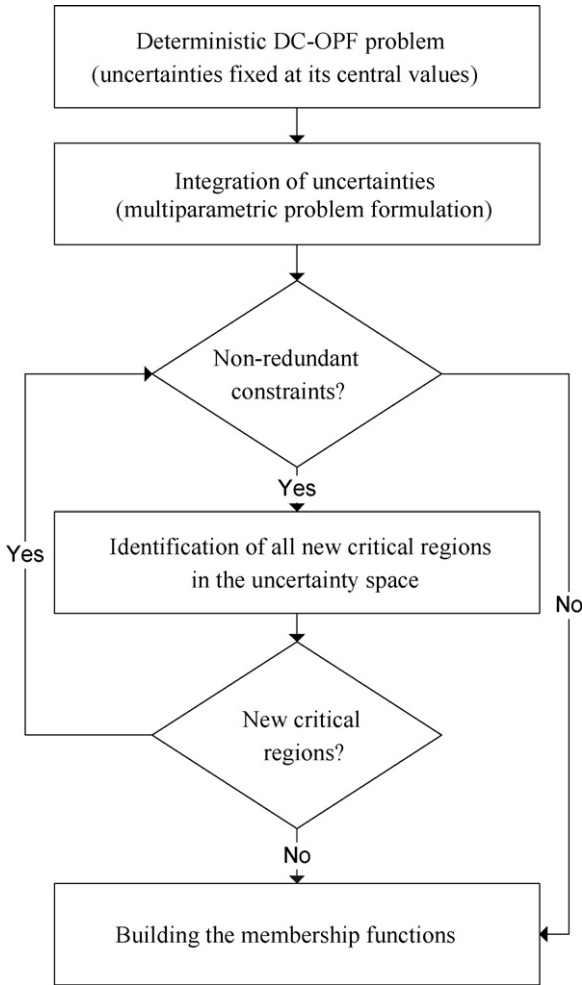


Fig. 3. New fuzzy DC optimal power flow algorithm.

For a better understanding of this procedure, Fig. 4 depicts the rectangles enclosing all load combinations between the “0.0” and “1.0-cuts” for a system supplying two trapezoidal fuzzy loads. In this figure, lines “a” and “b” represent constraints, for instance, related with branch flow or generator capacity limits, point O corresponds to the optimal and feasible solution of the initial deterministic DC OPF problem and the dashed lines define the range of values of the uncertainties at the *i*th level of the data membership functions. From Fig. 4, it becomes clear that non-redundant constraints, such as line “a”, can define any critical region such as R_i and R_j indicated in this figure. The process to identify these regions is implemented

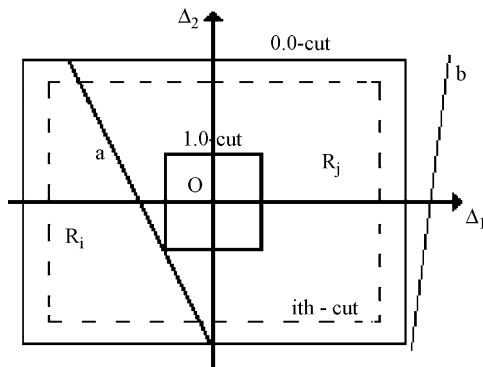


Fig. 4. Critical regions in the uncertainty space.

using the feasibility condition (19) described by the parameters of load vector uncertainties. In a systematic way, all critical regions are obtained by doing a dual pivoting over each of the optimal and feasible basis already identified.

In order to build the membership functions of the output variables (generations, branch flows and PNS), we must recall that, being a linear model, each variable in each critical region is represented by a linear expression. In this sense, if we are interested in capturing the widest possible behavior of a linear function $v(\Delta_1, \Delta_2)$ expressed in terms of the parameters Δ_1 and Δ_2 , we will then have to solve the problems (25)–(28).

$$\min_{\max} f = v(\Delta_1, \Delta_2) \quad (25)$$

$$\text{s.t. } k_{1i}\Delta_1 + k_{2i}\Delta_2 \leq b_i \quad (26)$$

$$\Delta_1^{\min \text{ ith cut}} \leq \Delta_1 \leq \Delta_1^{\max \text{ ith cut}} \quad (27)$$

$$\Delta_2^{\min \text{ ith cut}} \leq \Delta_2 \leq \Delta_2^{\max \text{ ith cut}} \quad (28)$$

In this problem, we are minimizing and maximizing a function $v(\Delta_1, \Delta_2)$ subjected to the constraints modelling the non-redundant conditions (26) together with the possible ranges of the input uncertainties regarding the *i*th cut under analysis (27) and (28). After solving this problem for several cuts, it is possible to build the membership function of v in this critical region. Once all critical regions are analyzed, the final membership function of v is obtained applying the fuzzy union operator to the partial membership functions obtained for that variable in order to guarantee that the final result displays the widest possible behavior given the specified uncertainties.

5.3. Integration of generation cost uncertainties

Let us now consider that at least one generation cost in vector c is modeled by a trapezoidal fuzzy number. Using a similar reasoning as the one adopted to consider demand uncertainties, we can formulate the multiparametric linear problem (29)–(31) in terms of the parameters Φ_k . In this formulation, Φ_{k1} and Φ_{k2} represent the range of values of the cost c_k regarding the 0.0 cut of the corresponding trapezoidal fuzzy number.

$$\min f = c(\Phi_k)^T \tilde{X} \quad (29)$$

$$\text{s.t. } A\tilde{X} \leq b \quad (30)$$

$$\Phi_{k1} \leq \Phi_k \leq \Phi_{k2} \quad (31)$$

The basic ideas behind the solution algorithm presented in Fig. 3 can still be used provided that some adaptations are made. In the first place, the algorithm starts by solving an initial deterministic DC OPF problem (4)–(8) for the crisp values of the fuzzy cost representations to identify a feasible and optimal solution. Following the same strategy, the linear multiparametric problem (32)–(36) is obtained including the parameters Φ_k used to model generation cost uncertainties.

$$\min f = \sum c_k(\Phi)Pg_k + G \sum \text{PNS}_k \quad (32)$$

$$\text{s.t. } \sum Pg_k + \sum \text{PNS}_k = \sum \text{Pl}_k^{\text{ctr}} \quad (33)$$

$$Pg_k^{\min} \leq Pg_k \leq Pg_k^{\max} \quad (34)$$

$$\text{PNS}_k \leq \text{Pl}_k^{\text{ctr}} \quad (35)$$

$$P_b^{\min} \leq \sum a_{bk}(Pg_k + \text{PNS}_k - \text{Pl}_k^{\text{ctr}}) \leq P_b^{\max} \quad (36)$$

In order to identify non-redundant constraints leading to the definition of the critical regions in the uncertainty space, we will now use the optimality condition (18) written in terms of the

parameters Φ_k . The identification of the critical regions is implemented performing a primal pivoting over the initial optimal and feasible basis as well as over all the new optimal and feasible basis identified along the search procedure.

When building the membership function of the output variables, we must recall that cost vector parametrization implies that the uncertainty space is partitioned in several regions. In each of these regions, there is an optimal basis associated with an optimal solution. This means that for each critical region of the multiparametric problem, the optimal basis is the same and so generations, branch flows and PNS remain the same inside that region. This also means that the values of these output variables will only change if there is a basis change, that is, if we move from one critical region to another.

Accordingly, for each critical region, the partial membership function of any variable is built using the non-redundant inequalities defining that region together with the maximum membership degree of the output variables. This is simple done solving the system formed by the linear inequalities that define each critical region to determine the point in the critical region under analysis having the largest membership degree. Once all partial membership function are built, we use the fuzzy union operator to aggregate all the results for the same variable to ensure that its final result displays the widest possible behavior in the specified uncertainty space.

5.4. Simultaneous integration of demand and generation cost uncertainties

Let us now consider that there are uncertainties affecting both elements of the cost and load vectors leading to the condensed problem (16) and (17). The solution algorithm presented in Fig. 3 remains valid, provided once again that some adaptations are made. In the first place, the initial deterministic DC OPF problems (4)–(8) are now run by substituting each fuzzy load and each fuzzy cost coefficient by their corresponding central values, PI_k^{ctr} and c_k^{ctr} , respectively. Once the optimal and feasible solution for this initial problem is obtained, the linear multiparametric problem (37)–(41) is built that integrate the load and the cost coefficient uncertainties in the initial optimization problem.

$$\min f = \sum c_k(\Phi)Pg_k + G \sum PNS_k \quad (37)$$

$$\text{s.t.} \quad \sum Pg_k + \sum PNS_k = \sum PI_k^{ctr} + \sum \Delta_k \quad (38)$$

$$Pg_k^{\min} \leq Pg_k \leq Pg_k^{\max} \quad (39)$$

$$PNS_k \leq PI_k^{ctr} + \Delta_k \quad (40)$$

$$P_b^{\min} \leq \sum a_{bk}(Pg_k + PNS_k - (PI_k^{ctr} + \Delta_k)) \leq P_b^{\max} \quad (41)$$

The process to identify non-redundant constraints is implemented using both the inequalities given by the optimality (18) and feasibility (19) conditions expressed as linear functions of the uncertainty parameters Φ_k and Δ_k , respectively. As a result of the increased number of parameters modelling data uncertainties, the search for all critical regions should be conducted in a more structured way. This leads to the adoption of a search tree as illustrated in Fig. 5, where ρ_i defines the index for the set of basic variables in a given critical region i .

Departing from one node in the tree, one can find two kinds of neighbor basis. The first one is determined by the application of the feasibility condition (19) (in Fig. 5, these bases correspond to nodes at the left of its departure node). The second type results from the optimality condition (18) (in Fig. 5, these bases correspond to nodes on the right of its departure node). This process is repeated for each new node until no non-redundant constraints

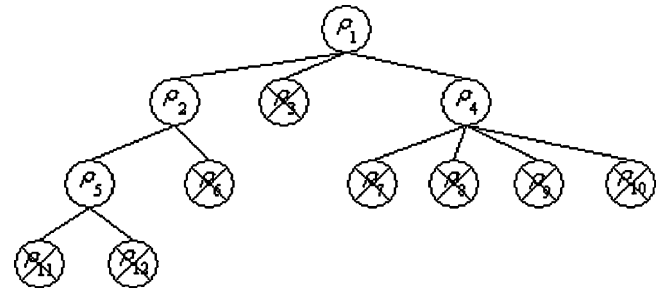


Fig. 5. Search tree to illustrate the search procedure.

exist or all the identified critical regions correspond to already known ones. In Fig. 5 and for illustration purposes, the crosses denote bases that are not new regarding previously identified ones. Similar to the algorithms described in Sections 5.2 and 5.3, each critical region is defined by a set of inequality conditions related, in this case, both with the feasibility and optimality conditions.

Once all critical regions are identified, the algorithm proceeds with the construction of the membership function of the final results. In order to do this, we once again recognize that in each region, the behavior of each variable is expressed by a linear expression and so, they are solved for each of them and for each critical region, optimization problems (25)–(28) to identify the widest possible behavior of that variable in that region. In this case, however, the number of constraints is larger given that we are now considering all the non-redundant inequalities given by (18) and (19). Finally, the partial membership functions built for each variable in each region are aggregated using the fuzzy union operator.

6. Case study

6.1. System data

The algorithms described in Sections 5.2–5.4 were used to build the membership functions of generations, branch flows and PNS considering a case study based on the IEEE 24 bus/38 branch test system. The original data for this system is given in reference [23]. Regarding data in this reference, the load was increased to 4456.83 MW, and Table 1 presents the central values of the loads in the system. The total installed capacity is 5800 MW according to the data in Table 2.

Branch data can be obtained from reference [23] considering that the transformers have a capacity of 400 MW, the capacity of the branches 1–6 and 8–13 was set at 175 MW and the capacity of the remaining branches was set at 500 MW.

6.2. Results considering only demand uncertainties

In the first place, we considered that all loads were affected by uncertainty represented by trapezoidal fuzzy numbers as the one depicted in Fig. 1. To build these numbers, we considered an

Table 1
Load central values.

Bus	Load (MW)	Bus	Load (MW)	Bus	Load (MW)
1	50.00	7	142.75	15	564.89
2	172.85	8	304.72	16	278.20
3	220.76	9	311.85	18	273.41
4	132.46	10	347.49	19	322.54
5	146.52	13	472.23	20	128.10
6	242.35	14	345.71	–	–

Table 2
Installed capacity in the system.

Bus/generator	Capacity (MW)	Cost (€/MWh)	Bus/generator	Capacity (MW)	Cost (€/MWh)
1/1	40.0	3.0	15/3	24.0	2.0
1/2	40.0	3.2	15/4	24.0	2.0
1/3	152.0	4.0	15/5	24.0	2.0
1/4	152.0	4.3	15/6	310.0	6.7
2/1	40.0	3.7	16/1	310.0	5.5
2/2	40.0	3.7	18/1	800.0	9.0
2/3	152.0	4.1	21/1	800.0	8.0
2/4	152.0	4.2	22/1	100.0	1.5
7/1	200.0	4.4	22/2	100.0	1.7
7/2	200.0	4.5	22/3	100.0	1.9
13/1	394.0	6.1	22/4	100.0	2.0
13/2	394.0	6.2	22/5	100.0	2.1
13/3	394.0	6.7	22/6	100.0	2.2
15/1	24.0	2.0	23/1	200.0	5.0
15/2	24.0	2.0	23/2	310.0	4.8

uncertainty range of $\pm 10\%$ at the 0.0 level and $\pm 5\%$ at the 1.0 cut regarding the central values in Table 1. After running the algorithm described in Section 5.2, we obtained the membership functions sketched in Figs. 6a and b and 7 for the generations at generators 1/4, 7/2, 15/6, 18/1 and 21/1. It should be mentioned that for the data referred above and for the load uncertainty ranges just specified, the branches 1–5 and 7–8 are at their capacity limit of 175 MW.

These results indicate that load uncertainties are essentially accommodated by generator 21/1, since it is the last one to be dispatched because of its higher variable cost (see Table 2) and by the generators 1/4 and 7/2 given that branches 1–5 and 7–8 are at their capacity limits. As expected, from Fig. 7 we can also see that when generator 21/1 is on limit, load variations are accommodated by generator 18/1 and so this one becomes the last one to be dispatched. The generation at the remaining generators is fixed, which means that despite load uncertainties there are a number of generators for which the generation values are not affected by those possible variations.

6.3. Results considering only generation cost uncertainties

In the second place, we considered that the variable cost of some generators was modelled by trapezoidal fuzzy numbers. In this case, we considered that the cost of generators 1/1, 1/3, 13/1, 18/1, 21/1

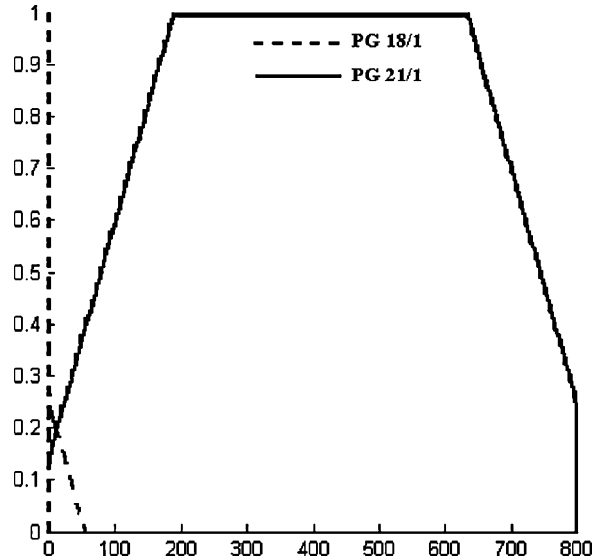


Fig. 7. Membership functions obtained for generators 18/1 and 21/1 (generation values in MW).

and 23/1 are described by the trapezoidal fuzzy numbers (42)–(47). It should be noticed that the central values of these trapezoidal fuzzy numbers coincide with the costs indicated in Table 2 for these generators.

$$CP_{G1/1} = (2.50; 2.85; 3.15; 3.50) \text{ €/MWh} \tag{42}$$

$$CP_{G1/3} = (3.25; 3.85; 4.15; 4.75) \text{ €/MWh} \tag{43}$$

$$CP_{G13/1} = (5.60; 6.00; 6.20; 6.60) \text{ €/MWh} \tag{44}$$

$$CP_{G18/1} = (7.80; 8.50; 9.50; 10.20) \text{ €/MWh} \tag{45}$$

$$CP_{G21/1} = (6.80; 7.75; 8.25; 9.20) \text{ €/MWh} \tag{46}$$

$$CP_{G23/1} = (4.60; 4.75; 5.25; 5.40) \text{ €/MWh} \tag{47}$$

Figs. 8a and b and 9a and b present the results obtained for these generators. These figures indicate that the membership functions include the generation values obtained for the initial deterministic DC OPF with 1.0 membership degree. This means that the values 152.0 MW for generators 1/3, 79.84 MW for generator 1/4, 0 MW for generator 18/1 and 411.24 MW for generator 21/1 belong to

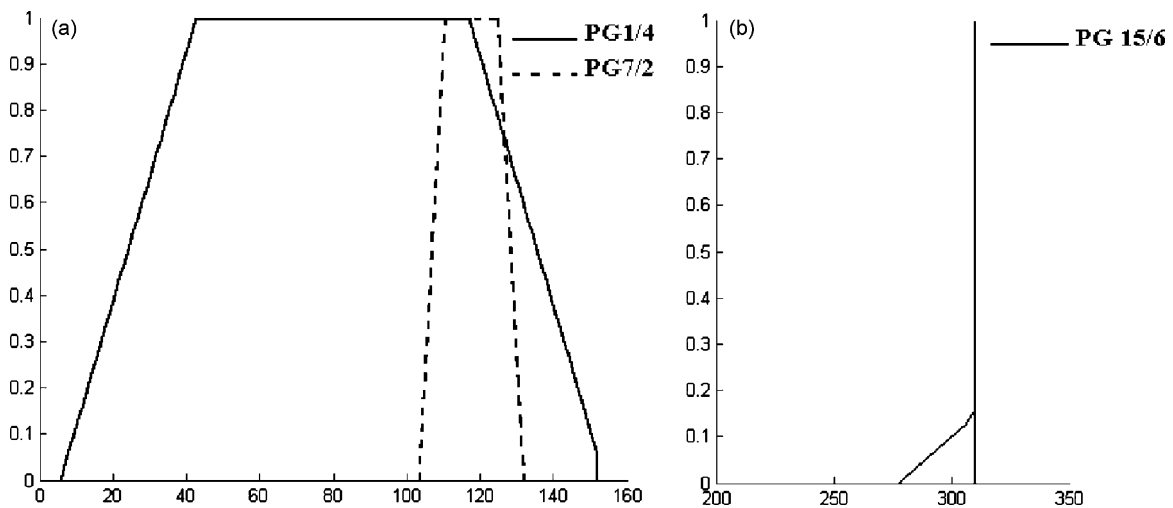


Fig. 6. Membership functions obtained for some generators: (a) generators 1/4 and 7/2 and (b) generator 15/6 (generation values in MW).

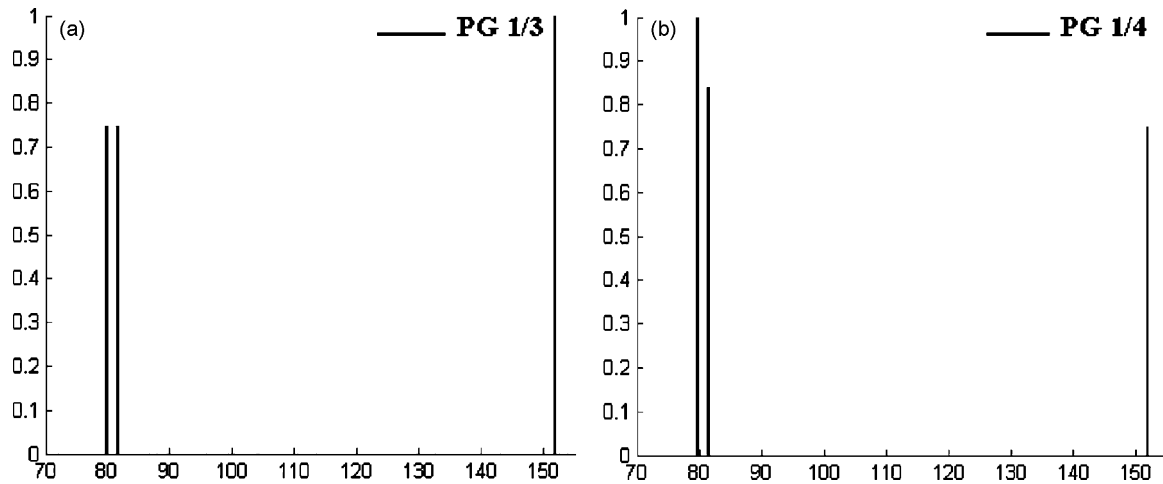


Fig. 8. Membership functions obtained for some generators: (a) generator 1/3 and (b) generator 1/4 (generation values in MW).

the membership functions of these generators, respectively. Then, due to different generation cost combinations determined by the specified cost uncertainties, there are different generation strategies leading to different values in each membership function. As an example in Fig. 8a, generator 1/3 can produce 79.84 or 81.56 MW with a credibility degree of 0.75 or 152.0 MW with a credibility degree of 1.0. Regarding this point, it must be emphasized that the membership function of generators 1/1, 13/1 and 23/1 are not here represented, since for the specified generation cost uncertainties and load scenario their generation levels did not exhibit any variation.

6.4. Results considering both demand and generation cost uncertainties

Similarly to what was described in Section 6.2, in this case, we also considered that all specified loads are represented by trapezoidal fuzzy numbers whose uncertainty range are of $\pm 10\%$ at the 0.0 level and $\pm 5\%$ at the 1.0 cut regarding the central values in Table 1. However, in this case, we also considered the generation cost uncertainties given by (42)–(47). After running the algorithm described in Section 5.4, we obtained the membership functions sketched in Figs. 10a, b and 11a, b for the generations at generators 1/3, 1/4, 7/2, 15/6, 18/1, 21/1 and 23/1. It should be mentioned that for the data referred above and for the specified uncertainty ranges, branches 1–5 and 7–8 are at their capacity limit of 175 MW.

Comparing these results with the ones presented in Figs. 6a and b and 7, we can see that some generators are affected by the specified cost uncertainties as, for instance, generators 1/3, 1/4, 18/1 and 21/1. Differently, some others as generators 7/2 and 15/6 are not affected by the specified cost uncertainties and so the membership functions obtained in Sections 6.2 and 6.4 are equal. In some other cases, as for instance, generator 23/1 in Fig. 10b, the membership function is affected neither by load uncertainties nor by cost uncertainties. This is a relevant and interesting result indicating that whatever are the combinations of load values and generator cost values, the output of some variables is fixed and it does not vary regarding the value that was initially obtained when running the deterministic DC OPF study.

Apart from that, the capacity limit of branch 1–5 constrains the output level of the generators located at bus 1, leading to membership functions displaying large possible variations. Due to this branch limit constraint, the most expensive generator in bus 1 (generator 1/3 or generator 1/4) has to reduce its output, so that the active flow constraint of branch 1–5 is enforced. From the specified generation cost uncertainties, it is also possible to conclude that there is a change regarding the system marginal generator, at least for some combinations of the specified costs. The membership functions of generators 18/1 presented in Fig. 11a and of generator 21/1 in Fig. 11b illustrate this fact, since for some combinations of the specified generation costs, the generator 18/1 becomes the sys-

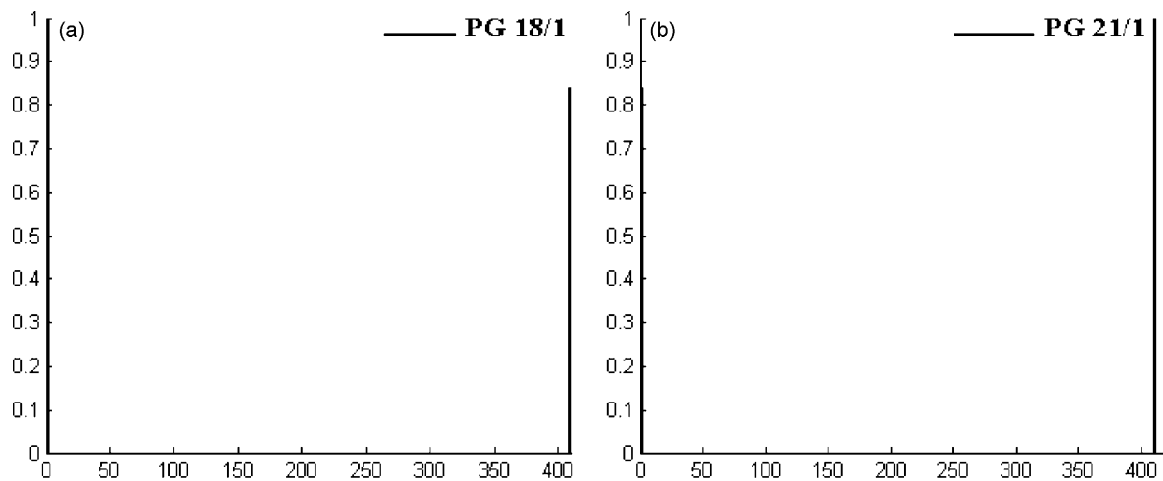


Fig. 9. Membership functions obtained for some generators: (a) generator 18/1 and (b) generator 21/1 (generation values in MW).

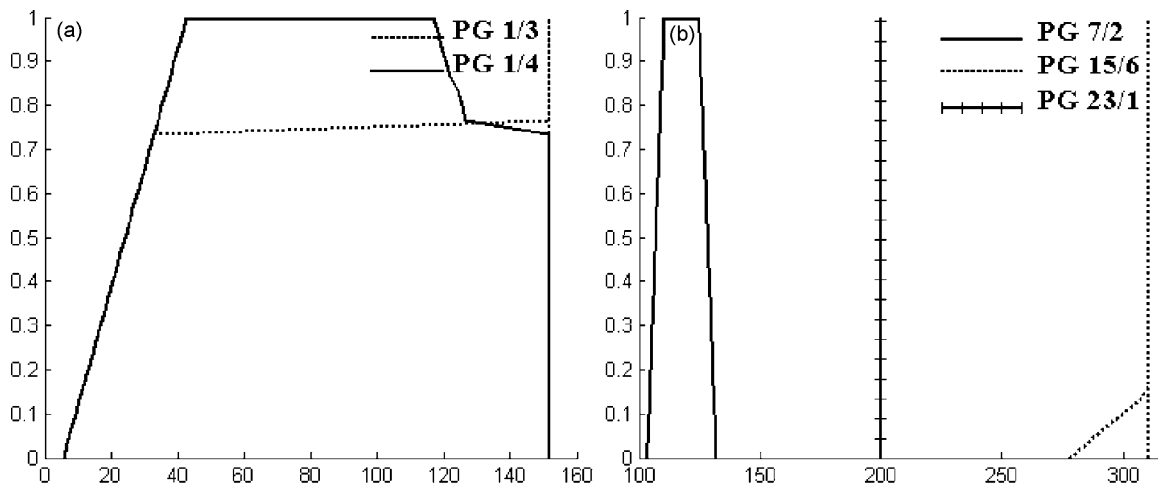


Fig. 10. Membership functions obtained for some generators: (a) generators 1/3 and 1/4 and (b) generators 7/2, 15/6 and 23/1 (generation values in MW).

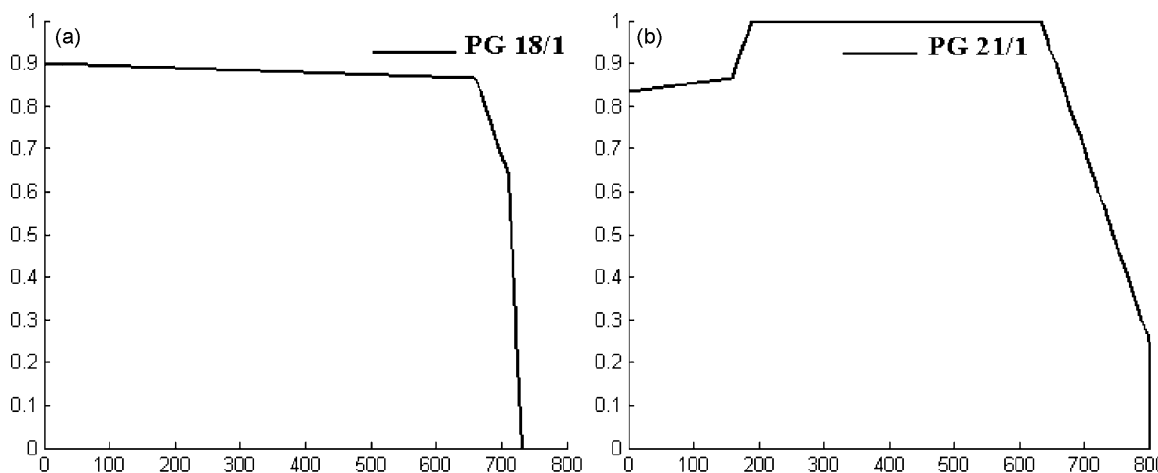


Fig. 11. Membership functions obtained for some generators: (a) generator 18/1 and (b) generator 21/1 (generation values in MW).

tem marginal generator, while for other combinations the marginal one is the generator 21/1.

7. Conclusions

In this paper, we formalized a new fuzzy DC optimal power flow approach and highlighted the main differences between this new approach and the original one developed back in the 1990s. As it was shown, this new approach accommodates not only load uncertainties represented by trapezoidal fuzzy numbers but also generation cost uncertainties or both of them, in a simultaneous way. Additionally, since this new approach is based on linear multiparametric programming techniques, it can present more accurate results than the algorithm originally conceived. These models and algorithms can be used by several entities and agents in the power sector namely to address expansion planning and operation planning problems in order to get more insight on the possible behavior of generations, branch flows and power not supplied reflecting data uncertainties modeled by fuzzy sets.

These features are especially interesting in the current very volatile and more unpredictable world in which this kind of tools will be very useful to map uncertainties on the results of optimization problems. Finally, it is also important to refer that this volatility and the more frequent change of patterns and assumptions reduces the history on system behavior. This ultimately means that the derivation and the use of probabilistic models will have to be done

in a more cautious way. This problem can enlarge the possibility of incorporating the knowledge of experts in several models so that formulations and algorithms as the ones described in this paper can play a more significant role in the future.

Acknowledgement

The first author would like to thank Fundação para a Ciência e Tecnologia, FCT, that funded this research work through the PhD grant n° SFRH/BD/34314/2006.

References

- [1] B. Borkowska, Probabilistic load flow, IEEE Trans. PAS PAS-93 (1974) 752–759.
- [2] R.N. Allan, B. Borkowska, C.H. Grigg, Probabilistic analysis of power flows, Proc. IEE 121 (1974) 1551–1556.
- [3] R.N. Allan, M.R.G. Al-Shakarchi, Probabilistic a.c load flow, Proc. IEE 123 (1976) 531–536.
- [4] R.N. Allan, C.H. Grigg, D.A. Newey, R.F. Simmons, Probabilistic power-flow techniques extended and applied to operation decision making, Proc. IEE 123 (1976) 1317–1324.
- [5] R.N. Allan, M.R.G. Al-Shakarchi, Probabilistic techniques in a.c load flow analysis, Proc. IEE 124 (1977) 154–160.
- [6] R.N. Allan, A.M. Leite da Silva, R.C. Burchett, Evaluation methods and accuracy in probabilistic load flow solutions, IEEE Trans. PAS PAS-100 (1981) 2539–2546.
- [7] R.N. Allan, A.M. Leite da Silva, Probabilistic load flow using multilinearisation, IEE Proc. 128 (Pt. C) (1981) 280–287.
- [8] A.M. Leite da Silva, V.L. Arienti, Probabilistic load flow by a multilinear simulation algorithm, IEE Proc. 137 (Pt. C) (1990) 256–262.

- [9] A.M. Leite da Silva, R.N. Allan, S.M. Soares, V.L. Arienti, Probabilistic load flow considering network outages, IEE Proc. 132 (Pt. C) (1985) 139–145.
- [10] T.S. Karakatsanis, N.D. Hatziaargyriou, Probabilistic constrained load flow based on sensitivity analysis, IEEE Trans. Power Syst. 9 (1994) 1853–1860.
- [11] P. Zhang, S.T. Lee, Probabilistic load flow computation using the method of combined cumulants and Gram–Charlier expansion, IEEE Trans. Power Syst. 19 (2004) 676–682.
- [12] M.E. El-Hawary, G.A.N. Mbalalu, Stochastic optimal load flow using a combined quasi-Newton and conjugated gradient technique, Electric Power Energy Syst. 11 (1989) 85–93.
- [13] M. Madrigal, K. Ponnambalam, V.H. Quintana, Probabilistic optimal power flow, in: Proceedings of the IEEE Canadian Conference on Electrical and Computer Engineering, Waterloo, Canada, 1998, pp. 385–388.
- [14] A. Schellenberg, W. Rosehart, J. Aguado, Cumulant-based probabilistic optimal power flow (P-OPF) with Gaussian and gamma distributions, IEEE Trans. Power Syst. 20 (2005) 773–781.
- [15] P.R. Gribik, D. Shirmohammadi, S. Hao, C.L. Thomas, Optimal power flow sensitivity analysis, IEEE Trans. Power Syst. 5 (1990) 969–976.
- [16] V. Miranda, M.A. Matos, J.T. Saraiva, Fuzzy load flow: new algorithms incorporating uncertain generation and load representation, in: Proceedings of the 10th PSCC, Butterworths, London, 1990.
- [17] V. Miranda, J.T. Saraiva, Fuzzy modelling of power system optimal load flow, IEEE Trans. Power Syst. 7 (1992) 843–849.
- [18] J.T. Saraiva, V. Miranda, L.M.V.G. Pinto, Impact on some planning decisions from a fuzzy modelling of power systems, IEEE Trans. Power Syst. 9 (1994) 819–825.
- [19] J.T. Saraiva, V. Miranda, L.M.V.G. Pinto, Generation/transmission power system reliability evaluation by Monte-Carlo simulation assuming a fuzzy load description, IEEE Trans. Power Syst. 11 (1996) 690–695.
- [20] J.T. Saraiva, V. Miranda, Identification of hedging policies in generation/transmission systems, in: Proceedings of the 12th Power Systems Computation Conference, PSCC, Dresden, Germany, 1996.
- [21] B.A. Gomes, J.T. Saraiva, Calculation of nodal marginal prices considering load and generation price uncertainties, in: Proceedings of the IEEE Lausanne Power Technology, Lausanne, Switzerland, 2007.
- [22] T. Gal, Postoptimal Analysis Parametric Programming and Related Topics, McGraw Hill, 1979.
- [23] Task Force of Application of Probabilistic Methods Subcommittee, IEEE Reliability Test System, IEEE Trans. PAS, PAS-98 (1979) 2047–2054.

Bruno André Gomes was born in Ovar, Portugal, in 1977. In 2001, he got his B.Sc. from the Faculdade de Ciências e Tecnologia da Universidade de Coimbra and in 2005 he got his M.Sc. from the Faculdade de Engenharia da Universidade do Porto, FEUP. Currently, he has a grant from the Fundação para a Ciência e Tecnologia, FCT, and he is completing his Ph.D. in FEUP.

João Tomé Saraiva was born in Porto, Portugal, in 1962. In 1987, 1993 and 2002, he got his M.Sc., Ph.D. and Agregado degrees, respectively, in Electrical and Computer Engineering from the Faculdade de Engenharia da Universidade do Porto, where he is currently professor. In 1985, he joined INESC Porto, where he was head researcher or collaborated in several projects related with the development of DMS systems, quality in power systems and tariffs for the use of transmission and distribution networks. Several of these projects were developed under consultancy contracts with the Portuguese Electricity Regulatory Agency.